Acta Crystallographica Section D
Biological Crystallography
ISSN 0907-4449

Structure of human muscle creatine kinase

Yue-quan Shen,[a] Liang Tang,[a] Hai-meng Zhou[b] and Zheng-jiong Lin[a]*

[a]National Laboratory of Biological Macromolecules, Institute of Biophysics, Academia Sinica, Beijing 100101, People's Republic of China, and [b]Department of Biological Science and Biotechnology, Tsinghua University, Beijing 100084, People's Republic of China

Correspondence e-mail: lin@sun5.ibp.ac.cn

Received 13 February 2001
Accepted 9 May 2001

PDB Reference: human muscle creatine kinase, 1i0e.

The crystal structure of human muscle creatine kinase has been determined by the molecular-replacement method and refined at 3.5 Å resolution. The structures of both the monomer and the dimer closely resemble those of the other known structures in the creatine kinase family. Two types of dimers, one with a non-crystallographic twofold symmetry axis and the other with a crystallographic twofold symmetry axis, were found to occur simultaneously in the crystal. These dimers form an infinite 'double-helix'-like structure along an unusual long crystallographic 3_1 axis.

1. Introduction

Creatine kinase (E.C. 2.7.3.2) reversibly catalyzes the phosphoryl transfer between ATP and creatine. It plays an important role in the rapid regeneration of ATP in cells and tissues with high and fluctuating energy demands. Two kinds of creatine kinases (CK) from cytosol and mitochondria have been isolated from many species. Cytosolic CK, a dimer of about 85 kDa, has three isoforms: MM, MB and BB (M and B denote muscle and brain tissues, respectively; Eppenberger *et al.*, 1967). However, mitochondrial CK has two isoforms, ubiquitous Mia-CK and sarcomeric Mib-CK, existing in dimeric and octameric forms (Schlegel, Wyss *et al.*, 1988; Schlegel, Zurbriggen *et al.*, 1988). An elevated level of CK in human blood is an important diagnostic indicator for diseases of the nervous system and the heart muscle, for malignant hypothermia and for certain tumours.

More than 20 creatine kinases have been sequenced (Muhlebach *et al.*, 1994) and they have high amino-acid sequence identity. Since 1996, several creatine kinase crystal structures have been solved, including mitochondrial CK from sarcomas (sMtCK; Fritz-Wolf *et al.*, 1996), MM-type CK from rabbit (RCK; Rao *et al.*, 1998), BB-type CK from chicken (BB-CK; Eder *et al.*, 1999) and mitochondrial CK from human (uMtCK; Eder, Fritz-Wolf *et al.*, 2000). These structural investigations have provided important information on the folding, active-site conformation and oligomeric states of the enzyme.

The MM-type creatine kinase from human muscle (HCK) was purified and characterized (Yang *et al.*, 1997; Yang & Zhou, 1997) and the gene was cloned, characterized and partially sequenced (Trask *et al.*, 1988). Here, we describe the crystal structure of HCK in the unliganded state at 3.5 Å resolution.

2. Materials and methods

The crystallization of and data collection from HCK were reported by Tang *et al.* (1998). The data were reprocessed with the *HKL* suite of programs (Otwinowski & Minor, 1997). The space group was reassigned as $P3_112$ or $P3_212$. The crystal has an unusual long cell dimension in the *c* direction (402.9 Å). The crystallographic asymmetric unit contains three or four monomers, corresponding to V_M values of 3.5 or 2.6 Å^3 Da^{-1} and solvent contents of 64.7 or 53.0%, respectively (Matthews, 1968).

The self-rotation function calculated using the program *POLARRFN* (Collaborative

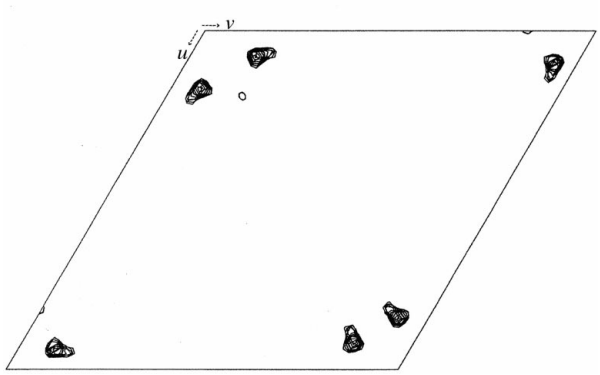

Figure 1
w = 0.25 section of the Patterson map calculated from the data set in the 10.0–4.0 Å resolution range. Contouring starts at the 4σ level; the interval is 1.5σ.

Computational Project, Number 4, 1994) did not yield any significant peaks. However, the Patterson map calculated in the 10.0–4.0 Å resolution range revealed a prominent peak with a height of 6.6% of the origin in the section w = 0.249 (Fig. 1). This result suggests that some or even all the monomers in the asymmetric unit had similar orientations and were separated by approximately 1/4 of the cell length along c.

The structure was solved by the molecular-replacement method (Rossmann & Blow, 1962) with the program *AMoRe* (Navaza, 1994). The structure of rabbit muscle creatine kinase determined at 2.4 Å (Rao *et al.*, 1998) with high sequence identity (∼96%) was selected as a search model. Residues with discrepant sequences were replaced with alanine. In the early stage of the molecular replacement, an angular step of 2° and data in the 8.0–4.0 Å resolution range were chosen to calculate the cross-rotation function. The results revealed only one significant peak. Three translation-function solutions (R, S, T) were then found from the same cross-rotation function peak. These three monomers had similar orientations. After rigid-body fitting, the model gave a correlation coefficient of 48.7% and an R factor of 45.3%. The electron-density map calculated on the basis of this model appeared to be reasonable. However, structural refinement using the *X-PLOR* program could not reduce the free R factor below 42%. Careful inspection of the crystal packing revealed that monomer R formed a dimer with the crystallographic twofold symmetry-related monomer R', as did monomer S with S'. These dimers were similar to those of other known structures in the creatine kinase family (Fritz-Wolf *et al.*, 1996; Rao *et al.*, 1998; Eder *et al.*, 1999). However, monomer T had no counterpart, suggesting that one monomer in the asymmetric unit may be lost. A hypothetical monomer, denoted by U, was then constructed so that U could form a dimer with T similar to the RR' or SS' dimers. Further analysis showed that U packs well into the unit cell without close contacts and also adopts an orientation similar to the other monomers.

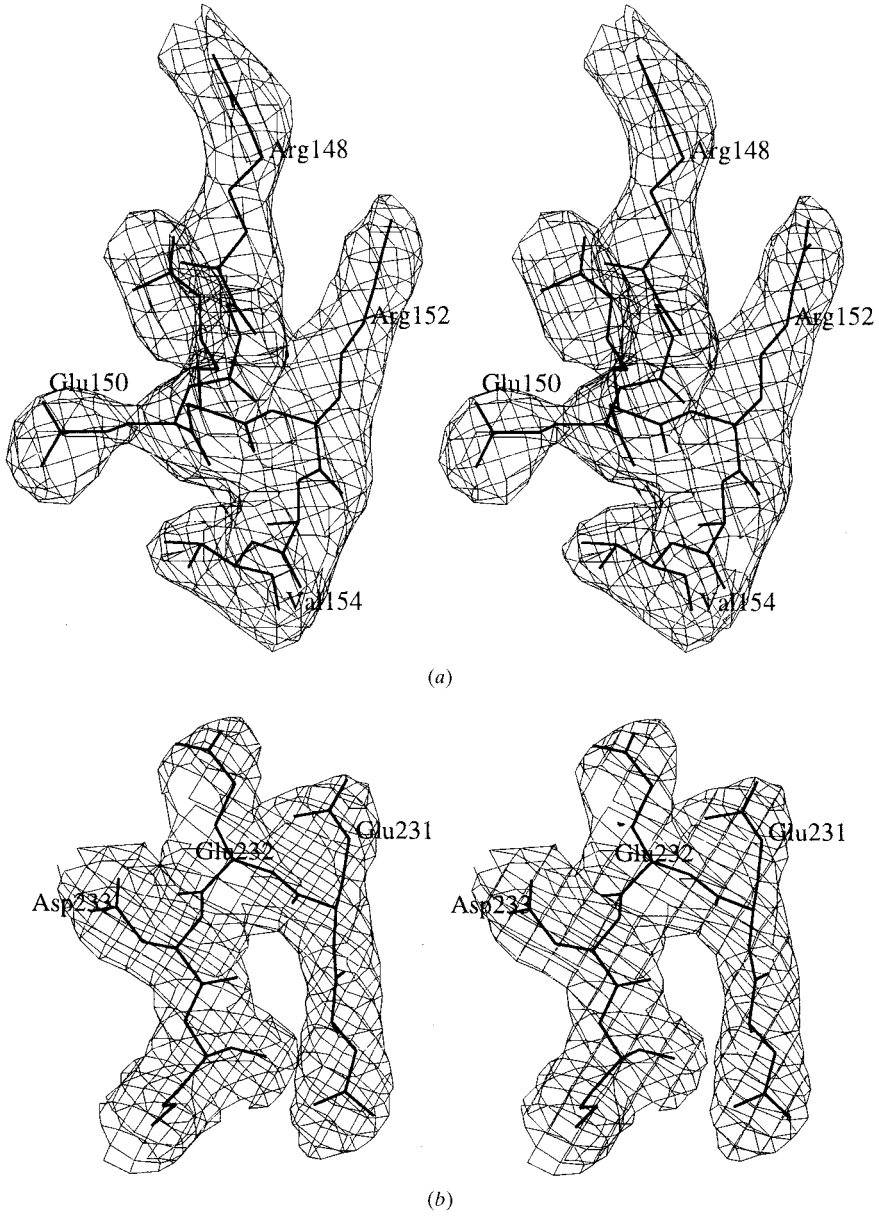

Figure 2
Omit maps for (*a*) fragment 148–154 located at the dimer interface and (*b*) the conserved negatively charged cluster (Glu231, Glu2232 and Asp233) which is essential for catalytic activity. The contour level is 3σ.

An attempt to find the fourth monomer by molecular replacement succeeded on using a finer angular step (1.2°) within the same resolution range. Under these conditions, a cross rotation-function calculation revealed one significant peak with a correlation coefficient of 16.8% (the maximum noise peak had a correlation coefficient of 8.5%) and the subsequent translation-function calculation based on the peak yielded four solutions corresponding to the positions of all four monomers (denoted R, S, T, U) in the asymmetric unit. The resulting model had a correlation coefficient of 58.8% and an R factor of 38.2% in the 8.0–4.0 Å resolution range after rigid-body fitting and was used for further refinement. The molecular replacement is summarized in Table 1. The space group was assigned as $P3_112$.

The structural refinement was carried out with data in the resolution range 8.0–3.5 Å without a cutoff using the program *CNS* (Brunger *et al.*, 1998). Model building was performed on an SGI workstation with the program *TURBO-FRODO* (Roussel & Cambillau, 1989). The refinement was carried out by a combination of positional refinement, simulated annealing and group B-factor refinement. In view of the low data resolution and the multiple copies of the monomers, non-crystallographic symmetry restraints were applied to each monomer (the positional weight constant and σ for the B factor were 450 kcal mol^{-1} Å^{-2} and 2.00 Å^2 for the main-chain atoms and 400 kcal mol^{-1} Å^{-2} and 3.00 Å^2 for the side-chain atoms; 1 kcal mol^{-1} Å^{-2} is equal to 4.184 kJ mol^{-1} Å^{-2}). During the refinement, the amino-acid sequence was gradually

changed to that of human creatine kinase. The final round of refinement converged to an R factor of 0.211 and a free R factor of 0.286 ($R_{\rm free}$ was calculated for 5% of randomly chosen reflections that were excluded from the refinement). A summary of the refinement statistics is shown in Table 2.[1]

3. Results and discussion

3.1. Model quality

The final model contains 11 608 non-H protein atoms, with standard deviations from stereochemistry of 0.008 Å for bond lengths and 1.34° for bond angles. In the Ramachandran plot, 76.4% of the non-glycine and non-proline residues are in the most favored regions, 22.9% are in the additional allowed regions and 0.6% are in the generously allowed regions. No residues are within the disallowed region.

In general, most residues have well defined corresponding electron densities in the final electron-density maps calculated with $2F_o - F_c$ coefficients (Fig. 2). Poor electron densities were observed for the N-terminal segment (residues 1–7) and the C-terminal surface loop (residues 321–331), so these were not included in the final model. Weak electron densities were also found for loops 65–70 and 183–205. It was reported that the latter three loops were all involved in rearrangements of the structure to shield the active site from water during the catalytic reaction procedure (Kabsch & Fritz-Wolf, 1997) and that these disordered loops might undergo substantial backbone movement (up to 15 Å) at the active site during binding of the transition-state analogue (Zhou *et al.*, 1998). Similar structural flexibility for these loops has been observed in other creatine kinases of known structure (Rao *et al.*, 1998; Eder *et al.*, 1999; Eder, Fritz-Wolf *et al.*, 2000).

3.2. Crystal packing

The four monomers in the asymmetric unit are denoted A, B, C, D ($A\leftrightarrow S$; $B\leftrightarrow U$; $D\leftrightarrow T$; $C\leftrightarrow R$; S, U, R, T: see Table 1). As described above, monomers A and B form a dimer AB with non-crystallographic twofold symmetry and monomer C (or D) forms a similar dimer but with a crystallographic twofold-axis related monomer C' (or D'). The molecular packing can be described as a 'double-helix' structure (Fig. 3). Two infinite protein helical chains were formed along the crystallographic 3_1 axis (the c axis) using the dimer as a building block and wound around each other. One chain uses dimer AB and its crystallographic equivalents as building blocks, while the other uses dimers CC', DD' and their crystallographic equivalents. However, the dominant interdimer interactions involve dimers from different chains, *e.g.* A–D' and B–C', using similar contact regions involving β-strand 171–175, turn 176–179 and turn 180–183. This region covers a buried surface area of 283 Å^2, as calculated using the program *SURFACE* (Collaborative Computational Project, Number 4, 1994).

3.3. Monomer and dimer structures

As expected, the monomer and dimer structures of HCK are similar to those of other creatine kinases, especially RCK. Superposition of the HCK and RCK (PDB code 2crk) monomers for 341 C$^\alpha$ atoms gives an r.m.s.d. value of 0.63 Å. This calculation does not include the three flexible segments (residues 65–70, 183–205 and 321–331). Significant differences between these two

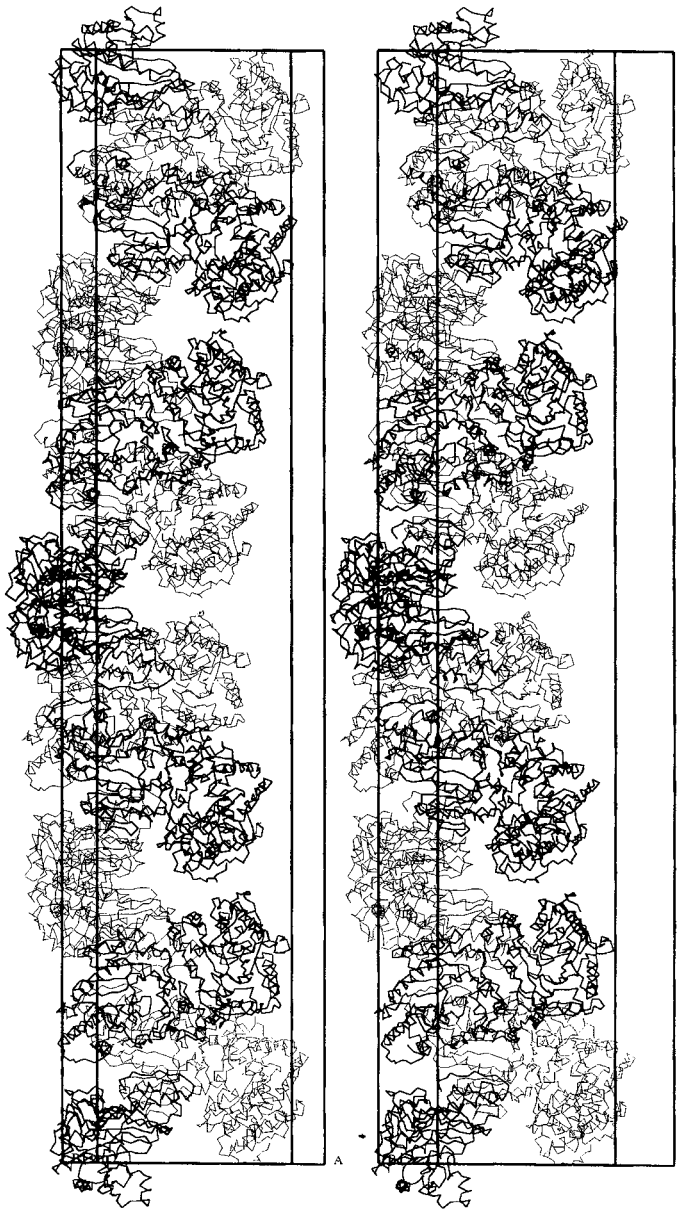

Figure 3
Double-helix-like crystal packing. Two infinite protein helical chains are formed along the crystallographic 3_1 axis (the c axis) using the dimer as a building block. Thin lines, using dimer AB and its crystallographic equivalents; thick lines, using dimers CC' and DD' and their crystallographic equivalents.

[1] Supplementary data have been deposited in the IUCr electronic archive (Reference: gr2148). Services for accessing these data are described at the back of the journal.

Table 1
Molecular replacement.

Corr, correlation coefficient; α, β, γ, Eulerian angles; x, y, z, fractional Cartesian coordinates. Values in parentheses are the highest noise peaks.

Cross-rotation function.

Peak number	α	β	γ	Corr
1	69.78	69.47	100.09	16.8 (8.6)

Translation function.

Peak number	x	y	z	Corr	R
1	0.96552	0.26075	0.48009	16.9 (14.0)	52.6 (53.6)

Fixed	Search	x	y	z	Corr	R
1	2	0.06189	0.18631	0.72830	25.9 (17.1)	50.9 (52.5)
1 + 2	3	0.16707	0.36529	0.97679	32.8 (25.6)	49.1 (50.5)
1 + 2 + 3	4	0.09388	0.45279	0.22638	36.2 (32.2)	48.3 (48.9)

Rigid-body fitting.

α	β	γ	x	y	z	Corr	R	Monomer
71.62	71.68	97.43	0.96666	0.25903	0.48017	58.8	38.9	*R*
68.71	72.66	102.87	0.06311	0.18529	0.72778	58.8	38.9	*T*
70.95	67.82	100.21	0.16949	0.36854	0.97677	58.8	38.9	*S*
72.99	66.29	95.53	0.09650	0.45512	0.22826	58.8	38.9	*U*

MM-type creatine kinases occur in three surface loops (63–72, 115–122 and 177–205). Because of the high homology of HCK to RCK, this result reflects the conformational flexibility of these loops. The superposition of the HCK and uMtCK (PDB code 1qk1) monomers for 313 C^{α} atoms without including the four obviously different regions (residues 8–14, 177–212, 319–329 and 368–381) gives an r.m.s.d. value of 1.03 Å. The largest differences between these two human-source creatine kinases are found in the N-terminus (residues 1–10 for uMtCK and residues 8–15 for HCK), a surface region (residues 171–203 for uMtCK and residues 176–208 for HCK) and the C-terminus (residues 367–379 for uMtCK and residues 372–381 for HCK). The N-terminus is most likely to be crucial for the octamerization of the Mt enzyme (Kaldis *et al.*, 1994; Eder, Fritz-Wolf *et al.*, 2000). The surface region undergoes a large movement during catalysis in all creatine kinases, as mentioned above. The C-terminus of the Mt enzyme may be related to mitochondrial membrane insertion (Schlattner *et al.*, 1998; Eder, Fritz-Wolf *et al.*, 2000).

The nucleotide-binding site consisting of the conserved positively charged arginine cluster (Arg96, 130, 132, 236, 292, 320 and 341) has a poorly defined electron density and higher *B* factor, indicating considerable side-chain flexibility, which can be explained by the absence of ATP or its analogues. The conserved negatively charged cluster (Glu231, Glu232 and Asp233) essential for catalytic activity as shown by site-directed mutagenesis experiments (Eder, Stolz *et al.*, 2000) has a well defined electron density (Fig. 2*b*) and shows an arrangement similar to RCK.

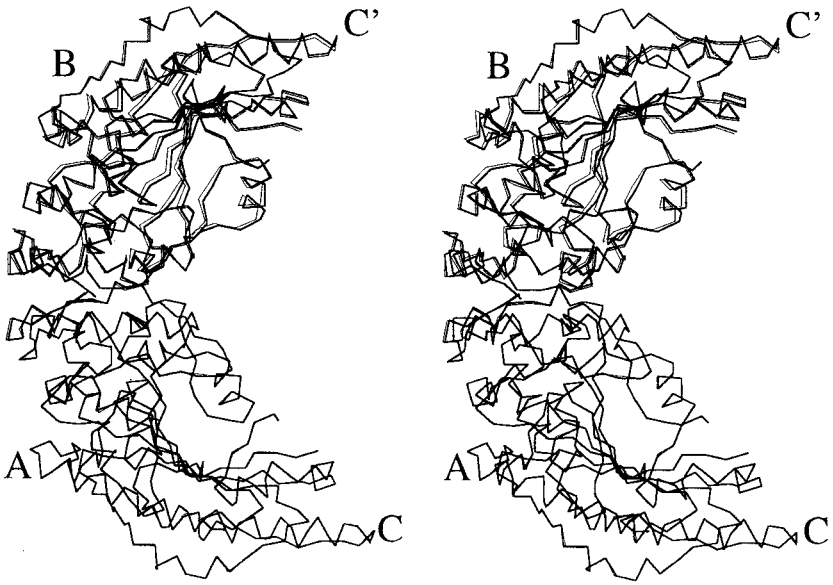

Figure 4
Comparison of *AB*- and *CC*′-type dimers after superposition of *A* and *C*.

Table 2
Data collection and structural refinement statistics.

Data collection	
Space group	$P3_112$
Unit-cell parameters (Å)	$a = b = 89.3$, $c = 402.9$
Number of monomers per asym. unit	4
Resolution range (Å)	30.0–3.5
No. of observations	63933
No. of unique reflections	21262
Completeness (outermost shell) (%)	88.3 (93.5)
$R_{\rm merge}$	0.118
Mosaicity	0.35
Structural refinement	
Resolution range (Å)	8.0–3.5
$R_{\rm work}$	0.211
$R_{\rm free}$	0.286
Current protein model	11604 protein atoms
R.m.s. deviations from ideal value	
Bond lengths (Å)	0.008
Bond angles (°)	1.3
Dihedral angles (°)	22.6
Improper angles (°)	0.83
Mean *B* values (Å^2)	
Protein atoms	41.4
Main-chain atoms	37.9
Side-chain atoms	44.9

All CK isoforms are known to form very stable dimers. The disintegration of the dimer into monomers only occurs under drastic conditions along with partial unfolding of the monomer (Gross *et al.*, 1995; Couthon *et al.*, 1997). This has been shown for all published CK crystal structures. In MM-type RCK, the dimer has a twofold crystallographic symmetry axis. However, in chicken mitochondrial Mib-CK, the dimer has a twofold non-crystallographic symmetry axis. Comparison of the two dimers revealed minor differences (Rao *et al.*, 1998). Interestingly, both types of dimers, one with a non-crystallographic symmetry axis (*AB*) and the other with a crystallographic symmetry axis (*CC*′ or *DD*′), were found to simultaneously occur in the structure of HCK presented here. The superposition of *AB* and *CC*′ or *DD*′ gives C^{α} r.m.s. deviations of 0.25 Å. A 1.43° rotation was required for the superposition of *B* onto *C*′ after a least-squares superposition of *A* onto *C* (Fig. 4). At the present resolution, it is not clear whether this minor difference implies hinge-bending flexibility of the dimer, probably induced by crystallographic effects, or is just a reflection of the experimental error.

The intermolecular interactions in dimer *CC*′ includes 22 hydrogen bonds, two salt bonds (Table 3) and a number of hydrophobic interactions. The residues involved in the intermolecular interactions include Asn8–Lys9, Tyr14, Glu18–Asp22, Lys25, Ser49, Asp54, Asp62, His145–Arg152, Lys177 and Arg209–Asp210. The intermolecular interactions in dimer *AB* are

Table 3
Intersubunit hydrogen bonds.

Distances greater then 3.5 Å are not given.

		Distances (Å)	
		Dimer *CC′*	Dimer *AB*
Glu18 O	Arg152 NH1	2.7	2.6
Glu19 OE1	Gly149 N	3.2	2.7
Glu19 OE1	Ser147 OG	2.7	2.6
Glu19 OE2	Ser147 OG	3.2	—
Glu19 OE2	Arg148 N	3.3	3.1
Glu19 OE2	Gly149 N	2.7	2.8
Glu19 O	Arg14 NH18	2.8	2.6
Tyr20 O	Arg152 NH1	—	3.0
Tyr20 O	Arg152 NH2	2.7	3.3
Asp54 OD1	Arg148 NH1	2.9	2.7
Asp54 OD1	Arg148 NH2	—	2.7
Gln58 NE2	Asp210 OD1	3.2	3.3
Asp62 OD1	Asp210 N	2.6	2.8
Arg152 NH1	Glu18 O	2.7	2.9
Arg149 N	Glu19 OE1	3.2	—
Ser147 OG	Glu19 OE1	2.7	2.6
Ser14 7OG	Glu19 OE2	3.2	3.1
Arg148 N	Glu19 OE2	3.3	—
Gly149 N	Glu19 OE2	2.7	2.8
Arg148 NH1	Glu19 O	2.8	3.0
Arg152 NH1	Tyr20 O	—	2.6
Arg152 NH2	Tyr20 O	2.7	—
Arg148 NH1	Asp54 OD1	2.9	2.9
Asp210 OD1	Gln58 NE2	3.2	3.1
Asp210 N	Asp62 OD1	2.6	2.6

similar to those in *CC′*, indicating the stability of the dimer interface. Moreover, comparison of RCK with uMtCK revealed that the interactions are also very similar in either the contact regions or the interaction number. In the HCK structure, the surface area buried by formation of the dimer is 2192 Å^2 for *CC′*, which is quite similar to the value (2200 Å^2) in uMtCK (Eder, Fritz-Wolf *et al.*, 2000) and corresponds to 6.7% of the monomer surface area. All these results support the view that the dimer in creatine kinase is well conserved.

We thank Professor Yasuo Hata in Kyoto University for his most helpful discussions. This work was supported by the China Natural Science Foundation (Grant No. 3900024).

References

Brunger, A. T., Adams, P. D., Clore, G. M., DeLano, W. L., Gros, P., Grosse-Kunstleve, R., Jiang, J.-S., Kuszewski, J., Nilges, M., Pannu, N. S., Read, R. J., Rice, L. M., Simonson, T. & Warren, G. L. (1998). *Acta Cryst.* D**54**, 905–921.
Collaborative Computational Project, Number 4 (1994). *Acta Cryst.* D**50**, 760–763.
Couthon, F., Clottes, E. & Vial, C. (1997). *Biochim. Biophys. Acta*, **1339**, 277–288.
Eder, M., Fritz-Wolf, K., Kabsch, W., Wallimann, T. & Schlattner, U. (2000). *Proteins*, **39**, 216–225.
Eder, M., Schlattner, U., Becker, A., Wallimann, T., Kabsch, W. & Fritz-Wolf, K. (1999). *Protein Sci.* **8**, 2258–2269.
Eder, M., Stolz, M., Wallimann, T. & Schlattner, U. (2000). *J. Biol. Chem.* **275**, 27094–27099.
Eppenberger, H. M., Dawson, D. M. & Kaplan, N. O. (1967). *J. Biol. Chem.* **242**, 204–209.
Fritz-Wolf, K., Schnyder, T., Wallimann, T. & Kabsch, W. (1996). *Nature (London)*, **381**, 341–345.
Gross, M., Lustig, A., Wallimann, T. & Furter, R. (1995). *Biochemistry*, **34**, 10350–10357.
Kabsch, W. & Fritz-Wolf, K. (1997). *Curr. Opin. Struct. Biol.* **7**, 811–818.
Kaldis, P., Furter, R. & Wallimann, T. (1994). *Biochemistry*, **33**, 952–959.
Matthews, B. W. (1968). *J. Mol. Biol.* **33**, 491–497.
Muhlebach, S. M., Gross, M., Wirz, T., Wallimann, T., Perriard, J. C. & Wyss, M. (1994). *Mol. Cell Biol.* **133**/**134**, 245–262.
Navaza, J. (1994). *Acta Cryst.* A**50**, 157–163.
Otwinowski, Z. & Minor, W. (1997). *Methods Enzymol.* **276**, 307–326.
Rao, J. K. M., Bujaca, G. & Wlodawer, A. (1998). *FEBS Lett.* **439**, 133–137.
Rossmann, M. G. & Blow, D. M. (1962). *Acta Cryst.* **15**, 24–31.
Roussel, A. & Cambillau, C. (1989). In *Silicon Graphics Geometry Partner Directory*, edited by Silicon Graphics. Mountain View, CA, USA: Silicon Graphics.
Schlattner, U., Forstner, M., Eder, M., Stachowiak, O., Fritz-Wolf, K. & Wallimann, T. (1998). *Mol. Cell. Biochem.* **184**, 125–140.
Schlegel, J., Wyss, M., Schurch, U., Schnyder, T., Quest, A., Wegmann, G., Eppenberger, H. M. & Wallimann, T. (1988). *J. Biol. Chem.* **263**, 16963–16969.
Schlegel, J., Zurbriggen, B., Wegmann, G., Wyss, M., Eppenberger, H. M. & Wallimann, T. (1988). *J. Biol. Chem.* **263**, 16942–16953.
Tang, L., Zhou, H.-M. & Lin, Z.-J. (1998). *Acta Cryst.* D**55**, 669–670.
Trask, R. V., Strauss, A. W. & Billadello, J. J. (1988). *J. Biol. Chem.* **263**, 17142–17149.
Yang, H. P., Zhong, H. N. & Zhou, H. M. (1997). *Biochim. Biophys. Acta*, **1338**, 147–150.
Yang, H. P. & Zhou, H. M. (1997). *Biochem. Mol. Biol. Int.* **43**, 1297–1304.
Zhou, G., Somasundaram, T., Blane, E., Parthasarathy, G., Ellington, W. R. & Chapman, M. S. (1998). *Proc. Natl Acad. Sci. USA*, **95**, 8449–8454.